 CMES, vol.50, no.1, pp.47-65, 2009

The Temperature-Quantum-Correction Effect on the MD-Calculated Thermal Conductivity of Silicon Thin Films

Tai-Ming Chang[1], Chien-Chou Weng[1], Mei-Jiau Huang[1]
Chun-Kai Liu[2] and Chih-Kuang Yu[2]

Abstract: We employ the non-equilibrium molecular dynamics (NEMD) simulation to calculate the in-plane thermal conductivity of silicon thin films of thickness 2.2nm and 11nm. To eliminate the finite-size effect, samples of various lengths are simulated and an extrapolation technique is applied. To perform the quantum correction which is necessary as the MD simulation temperature is lower than Debye temperature, the confined phonon spectra are obtained in advance via the EMD simulations. The investigation shows the thermal conductivities corrected based on the bulk and thin-film phonon densities of states are very close and they agree excellently with the theoretical predictions of a certain surface roughness. Those uncorrected or corrected by the Debye DOS on the other hand fail in capturing the variation trend of the thermal conductivity against the temperature.

Keywords: Non-equilibrium Molecular Dynamics, Lattice thermal conductivity, Silicon thin film, Finite-size effect, Quantum correction.

1 Introduction

In the past decades, much attention has been attracted to the thermal behavior of low-dimensional materials such as nanowire or thin-film structures because of the demand for miniaturization of electronic devices. The reduced feature sizes lead to an increase in heat dissipation density and cause failure in operation. Alternatively, it was also found that these low-dimensional materials provide desirable thermal properties for possible improvements of thermoelectric devices. It is well known that the application of a thermoelectric device is limited by its poor efficiency, which in turn is limited by the material figure-of-merit, $Z = S^2\ \sigma_e k$ (S is the

[1] Department of Mechanical Engineering, National Taiwan University, Taipei, Taiwan
[2] Electronics & Optoelectronics Research Laboratories, Industrial Technology Research Institute, Taiwan

Seebeck coefficient, σ_e is the electric conductivity, and k is the thermal conductivity). Recently, it was found experimentally as well as theoretically (Capinski, Cardona, Katzer, Maris, Ploog, and Ruf, 1999; Venkatasubramanian, Siivola, Colpitts, and O'Quinn, 2001; Cahilla, Ford, Goodson, Mahan, Majumdar, Maris, Merlin, and Phillpot, 2004) the low-dimensional materials such as quantum well, quantum wire, and superlattice structures have ZT value much larger than their bulk counterparts. The increase in ZT is attributed mainly to the reduced thermal conductivity, which is caused by the confinement size effect and the boundary/interface scattering. Hence, lots of studies have been performed to explore the phonon behavior in the semiconductor under the size effect.

To date, several theoretical models (Balandin, Wang, 1998; Chen, 1998; Khitun, Balandin, and Wang, 1999; Zou, Balandin, 2001; Huang, Chong, Chang, 2006; Huang, Chang, Chong, Liu, and Yu, 2007) have been proposed to predict the thermal conductivity of low-dimensional semiconductors. These investigations are mostly built on the phonon Boltzmann transport equation (PBTE) under the single-relaxation-time approximation. Usually a specularity parameter is introduced to characterize the strength of boundary scattering or the surface roughness. Empirical or semi-empirical equations are needed in order to evaluate various scattering mechanisms. To avoid those ad hoc models, the molecular dynamics (MD) that directly simulates the motion of atoms without any assumptions is a natural choice. Given a proper interatomic potential and the initial positions and velocities of atoms, MD traces the atomic trajectories by Newton's second law. This numerical method has been widely utilized for many nanoscale applications, such as in exploring the mechanical or thermal properties of nanostructures (Chen, Cheng, Hsu, 2007; Chakrabarty and cagin, 2008), nanoindentation of thin films (Nair, Farkas, Kriz, 2008; Liu, Tsai, 2009), water flow in a nanotube (Tang, Advani, 2007), and so on. For analyzing thermal properties, two different kinds of MD simulations, the equilibrium MD (EMD) (Volz, Chen, 1999; Volz, Chen, 1999; Volz, Saulnier, Chen, and Beauchamp, 2000; Zhong, Wang, and Xu, 2004; Gomes, Madrid, and Amon, 2004; Gomes, Madrid, Goicochea, and Amon, 2006; Landry, McGaughey, and Hussein, 2006) and the non-equilibrium MD (NEMD) (Jund, Jullien, 1999; Lukes, Li, Liang, and Tien, 2000; Schelling, Phillpot, Keblinski, 2002; Imamura, Tanaka, Nishiguchi, Tamura, and Maris, 2003; Feng, Li, and Guo, 2003; Wang, Li, 2006; Stevens, Zhigilei, and Norris, 2007; Miyazaki, Nagai, and Tsukamoto, 2008), have been developed. In the EMD approach, the thermal conductivity is calculated based on the fluctuation-dissipation theorem or the Green-Kubo relation. In NEMD approaches, either a constant heat flux or constant boundary temperatures are imposed on the simulation cell, statistically averaged temperature gradients are next calculated, and the thermal conductivity is finally determined by applying the

Fourier's law. A comparison between these two approaches can be found in the work of Schelling, Phillpot, and Keblinski (2002).

When low-dimensional materials such as thin-film or nanowire structures are studied by using the MD method, one sometimes has to worry about the evaporation of surface atoms. In the literature, three strategies have been proposed, including unconstrained free surfaces (Volz, Chen, 1999; Lukes, Li, Liang, and Tien, 2000), constrained surfaces with a few layers of fixed atoms (Lukes, Li, Liang, and Tien, 2000; Feng, Li, and Guo 2003), and a use of a surface potential (Gomes, Madrid, and Amon, 2004; Gomes, Madrid, Goicochea, and Amon, 2006). Films with unconstrained free surfaces take a long transient time to reach stationary and obtain the minimum surface potential energy. Besides, the crystal may collapse when systems are at very high temperatures. The second strategy makes sure no evaporation of surface atoms but surface atoms cannot rearrange themselves to obtain the minimum surface potential energy. Gomes, Madrid, and Amon (2004) proposed a use of the surface potential to impose an inward normal force on the surface atoms. Surface atoms were thus prevented from evaporation but allowed to rearrange (Aono, Hou, Oshima, and Ishizawa, 1982).

As far as thin films are concerned, Zhong, Wang, and Xu (2004) adopted the Lennard-Jones potential and calculated both in-plane and cross-plane thermal conductivities of thin films with free surfaces via EMD. They found the cross-plane thermal conductivity varies significantly with the film thickness. Gomes, Madrid, Goicochea, and Amon (2006) also adopted EMD to simulate the silicon thin film of thickness ranging from 2 nm to 217 nm at T=300K$\sim$1000K. They also observed anisotropic thermal conductivities, particularly when the film is extremely thin. Besides, they found the cross-plane thermal conductivity depends linearly on the film thickness and is nearly temperature-independent for temperature close to or above Debye temperature. Lukes, Li, Liang, and Tien (2000) calculated the cross-plane thermal conductivity of argon against the film thickness via NEMD. It was reported there is no observable difference in thermal conductivity between free- and fixed-surface thin films. Feng, Li, and Guo (2003) simulated cross-plane thermal conductivity of silicon thin film at T=500 K. A significant size effect and a linear dependence of the thermal conductivity on the film thickness ranging from 2 nm to 32 nm were observed once again. Wang and Li (2006) simulated films (2.715 nm $\sim$ 54.3 nm) at T=300K. The calculated thermal conductivities agreed with theoretical predictions corresponding to thinner films nonetheless.

Although the MD tools have been applied widely and successfully, several difficulties have to be overcome. First of all, one needs to worry about the finite-size effect. When the simulation cell is not sufficiently long, phonons may travel between the boundaries without suffering any scattering and the vibration wavelength

has a numerical upper bound. To eliminate the finite-size effect, a tremendously large system size is necessary. Alternatively, Schelling, Phillpot, and Keblinski (2002) proposed to obtain the desired thermal conductivity by extrapolating from those of finite-size systems according to the kinetic theory. Besides the finite-size effect, the quantum correction is essential as well. When the system temperature is lower than the Debye temperature or when not all phonon modes are excited, it becomes improper to define the local temperature according to the equipartition principle. The so-called quantum correction is to find out in some way according to the quantum theory the real temperature that corresponds to the system energy. The phonon dispersion relation or density of states (DOS) is usually required in correction and the most commonly used ones are the Debye DOS (Feng, Li, and Guo, 2003; Wang, Li, 2006). Gomes, Madrid, Goicochea, and Amon (2006) constructed the phonon DOS based on the experimentally measured bulk specific heat instead. That directly calculated from the lattice dynamics was also tried. Low-dimensional materials nonetheless possess different phonon spectra due to the size confinement effect (Zou, Balandin, 2001; Huang, Chong, Chang, 2006; Huang, Chang, Chong, Liu, and Yu, 2007). To the authors' knowledge, there has been no study that investigates the thermal transport in solids by taking all factors, such as the reliable potentials, the finite-size effect, the quantum correction, and the confined phonon spectra, into consideration. And this constitutes the motivation of the present work.

In this work, we attempt to apply the NEMD approach to study the in-plane thermal conductivity of silicon thin films. The Stillinger-Weber (SW) interatomic potential and the surface potential proposed by Gomes, Madrid, and Amon (2004) are selected. Two film thicknesses, 2.2 nm and 11 nm, are investigated and their lattice thermal conductivities against the temperature are targeted. The finite-size effect is eliminated by extrapolating the desired from those of finite-size systems (Schelling, Phillpot, and Keblinski, 2002). Most of all, we manage to obtain the confined phonon spectra via EMD simulations. Finally, due to the large number of atoms in problem, the computations in the present study are parallel processed by taking advantage of the spatial decomposition technique (Plimpton, 1995).

2 Computational methodology

2.1 Atomic potential models

MD simulations start from selecting a suitable potential function to describe the interaction among atoms. Most potential models were built based on Born-Oppenheimer approximation (Born, Oppenheimer, 1927), which separates the motion of the electron from the motion of the nuclei. For the interaction between neutral atoms (noble gases) and diatomic molecules, the commonly used potential models are

Lennard-Jones potential (Jones, 1924) and Morse potential (Morse, 1929) respectively. For silicon, several potential models have been developed in literatures such as Stillinger-Weber (SW) potential (Stillinger, Weber, 1985), Tersoff potential (Tersoff, 1986), and modified embedded atoms methods (MEAM) (Baskes, 1987). In the present study we adopt the SW potential because it can accurately predict many of thermal properties, such as thermal expansion coefficient and melting temperature. The SW potential contains two- and three-body potentials to maintain the diamond structure of Si, which are

$$\phi_2(r_{ij}) = \varepsilon \cdot A\left[Br_{ij}^{-p} - r_{ij}^{-q}\right] \cdot \exp\left(\frac{1}{r_{ij} - r_c}\right) \tag{1}$$

and

$$\phi_3(r_{ij}, r_{ik}, \theta_{jik}) = \varepsilon \cdot \lambda \cdot \exp\left[\frac{\gamma}{r_{ij} - r_c} + \frac{\gamma}{r_{ik} - r_c}\right] \times \cos\left(\theta_{jik} + \frac{1}{3}\right) \tag{2}$$

respectively, where r_{ij} is the distance between the atoms i and j, r_c is the cut-off radius, and θ_{jik} is the angle between $\vec{r}_{ij}$ and $\vec{r}_{ik}$. Note all the distances have been normalized by the characteristic length (σ=0.20951 nm) of silicon. The corresponding two- and three-body forces acting on the atom i are

$$\vec{F}_{ij} = \frac{\varepsilon \cdot A}{\sigma}\left[\left(pBr_{ij}^{-p-1} + qr_{ij}^{-q-1}\right) + \left(Br_{ij}^{-p} - r_{ij}^{-q}\right)\frac{1}{(r_{ij} - r_c)^2}\right] \cdot \exp\left(\frac{1}{r_{ij} - r_c}\right)\frac{\vec{r}_{ij}}{r_{ij}} \tag{3}$$

and

$$\vec{F}_{jik} = -\varepsilon\, \nabla_i\left[\phi_3(r_{ij}, r_{ik}, \theta_{jik}) + \phi_3(r_{ji}, r_{jk}, \theta_{ijk}) + \phi_3(r_{ki}, r_{kj}, \theta_{ikj})\right] \tag{4}$$

Values of the characteristic energy ε and other parameters used herein are extracted from the literature (Stillinger, Weber, 1985): ε=2.315eV, A=7.049556277, B=0.6022245584, p=4, q=0, λ=21, γ=1.2, and r_c=1.8.

On the other hand, the surface potential is (Gomes, Madrid, and Amon, 2004; Gomes, Madrid, Goicochea, and Amon, 2006)

$$\phi_w(d_w) = \frac{\varepsilon_w}{d_w^4} \cdot \exp\left(\frac{1}{d_w - r_{cw}}\right) \tag{5}$$

where ε_w (=9.2eV) is the characteristic surface potential energy, r_{cw} (=1.26) is the cut-off distance, and d_w (=r_{cw} initially) is the distance between an atom and a reference plane. The reference plane is initially set parallel to the film and at a distance

r_{cw} away from the surfaces of the film. An inward normal force is imposed on the atom whenever $d_w \leq r_{cw}$, namely

$$F_w(d_w) = \phi_w \cdot \frac{1}{\sigma}\left(\frac{4}{d_w} + \frac{1}{(d_w - r_{cw})^2}\right) \tag{6}$$

Surface atoms are thus prevented from evaporating. Finally, according to the Newton's second law

$$m_i \vec{a}_i = \vec{F}_i = \sum_{j \neq i}^{N} \vec{F}_{ij} + \sum_{j,k \neq i}^{N} \vec{F}_{jik} + \vec{F}_w \tag{7}$$

where m_i is the mass of the atom i and $\vec{a}_i$ is its instantaneous acceleration.

2.2 NEMD approach

Figure 1 is a schematic diagram of the simulated cell, which has a dimension of $L_x \times L_y \times L_z$ with the z direction being (001). Periodic boundary conditions are imposed in the y and z (in-plane) directions and surface potential is applied in the x (cross-plane) direction. To generate a constant heat flux in the system, the velocity-rescaling algorithm suggested by Jund and Jullien (1999) is employed. An amount of heat $\Delta\varepsilon$ is added in a region of thickness δ centered at $z = -L_z/4$ (source region) and removed from a region of same thickness centered at $z = -L_z/4$ (sink region) at every simulation time step. When the system achieves stationary, the heat current can be estimated, with Δt being the MD time increment, as

$$J_z = \frac{\Delta\varepsilon}{2L_x L_y \Delta t} \tag{8}$$

A too large or too small value of $\Delta\varepsilon$ causes significant noises in the simulation. Schelling, Phillpot, and Keblinski (2002) suggested a proper amount of $1 \times 10^{-4}\ eV/nm^2$. We next divide the simulation domain into many thin slices along the z-direction. In accordance with the equipartition principle, the instantaneous temperature in each slice is defined as

$$T_{MD}(z,t) = \sum_{i=1}^{N_{xy}} m v_i^2 \Big/ 3N_{xy}k_B \tag{9}$$

where m is the atomic mass, k_B is the Boltzmann constant, and N_{xy} is the total number of atoms in the slice.

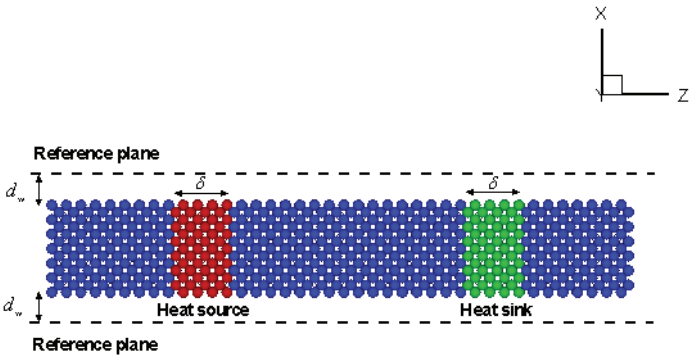

Figure 1: A schematic diagram of the simulated thin-film system.

2.3 Quantum correction

It is known that Eq.(9) is not a proper definition for the local temperature when the temperature is lower than the Debye temperature (θ_{Debye}). To make correction, one can look for the real temperature (T) by equating the slice energy from the quantum description to the simulated one (Lee, Biswas, Soukoulis, Wang, Chan, and Ho, 1991; Li, Porter, and Yip, 1998; Che, Cagin, Deng, and Goddard, 2000; Feng, Li, and Guo, 2003; Wang, Li, 2006; Gomes, Madrid, Goicochea, and Amon, 2006, McGaughey and Kaviany, 2006), that is

$$3N_{xy}k_BT_{MD} = \int_0^{\omega_D} D(\omega)\left[n(\omega,T)+1/2\right]\hbar\omega d\omega \tag{10}$$

where $D(\omega)$ is the phonon DOS,$n(\omega,T)$ is the equilibrium phonon distribution, ω is the phonon frequency, and $\hbar\omega/2$ is the zero-point energy. Commonly used DOS is the bulk DOS or the DOS calculated according to the Debye model. Previous theoretical investigations however have shown the phonon spectra of low dimensional materials such as nanowire (Zou, Balandin, 2001; Huang, Chong, Chang, 2006) and thin film (Huang, Chang, Chong, Liu, and Yu, 2007) differ from the bulk one. For instance, the elastic continuum model predicts discrete, instead of continuous, vibration modes in the finite dimension(s). In the present study, for consistence, we desire the confined phonon spectra of thin films which are obtained by an EMD approach as described below.

There are many existing methods for obtaining the phonon dispersion relations, such as by measuring the autocorrelation function of atomic velocity (Heino, 2007), of the displacement of atomic vibration (Trubitsyn, Dolgusheva, 2007; Miyazaki, Nagai, and Tsukamoto, 2008), or of the atomic positions (Dickey, Paskin, 1969).

After several tests, we found the method proposed by Dickey and Paskin (1969) can generate physically reasonable phonon spectra for Si and can be easily implemented. This method starts from calculating the normal coordinates of a periodic crystal under the harmonic assumption, namely

$$\alpha_q(t) = \sum_i \vec{r}_i(t) \cdot \vec{e}_q \cos\left(\vec{q} \cdot \vec{l}_i\right) \tag{11}$$

where $\vec{r}_i$ is the instantaneous position of atom i, $\vec{l}_i$ is the position of the lattice point, and $\vec{q}$ is the wave vector of interest. The atomic vibration, however, is anharmonic under the SW potential so that the α_q in Eq.(11) is not linearly independent. Therefore, a sufficiently long simulation time is thus necessary to distinguish the characteristic frequency ω_q from the Fourier analysis of the signal $\alpha_q(t)$ (Papanicolaou, Lagaris, Evangelakis, 1995).

The phonon density of states can be obtained at the same time by measuring the velocity autocorrelation function and taking a cosine Fourier transform (Papanicolaou, Lagaris, Evangelakis, 1995; Miyazaki, Nagai, and Tsukamoto, 2008) as follows

$$\frac{D(\omega)}{3N} = \frac{2}{\pi} \frac{\int_0^\infty \left\langle \sum_i v_i(t+\tau) \cdot v_i(\tau) \right\rangle \cos(\omega t)\, dt}{\left\langle \sum_i v_i^2(\tau) \right\rangle} \tag{12}$$

where N is the total number of atoms in the equilibrium system.

3 Results and discussions

3.1 Temperature distribution

In the present study, two thin films having a cross section of $L_x \times L_y = 4a_0 \times 4a_0$ and $20a_0 \times 20a_0$ respectively are investigated, where a_0 is the lattice constant of silicon, slightly depending on the temperature (Yim, Paff, 1974). The corresponding film thicknesses are about 2.2 nm and 11 nm respectively. The values of $\Delta\varepsilon$ are chosen to be 5×10^{-4} eV and 1.25×10^{-2} eV so that values of $\Delta\varepsilon/A$ are both close to 1×10^{-4} eV/nm^2. Moreover, we set the width δ=1.2nm. The thickness of each slice is about 0.14 nm. There are thus approximately 32 and 800 atoms in each slice of the thin films. The simulation time step adopted in the present study is 0.55 fs (Schelling, Phillpot, and Keblinski, 2002).

At the beginning of the simulation, atoms are set in a perfect diamond structure at some initial temperature $T_{MD,i}$. The velocity rescaling technique is next applied to

maintain the whole system at the prescribed temperature. The addition and depletion of energy are not imposed until the system is stabilized.

To reduce the statistical fluctuations, the slice temperatures are averaged over sufficiently many time steps (M) after the heat flow is evoked and the system becomes stationary again. The time-averaged temperature is calculated as follows

$$\langle T_{MD}(z)\rangle_M = \frac{1}{M}\sum_{m=0}^{M-1} T_{MD}(z, t_{N_t-m}) \tag{13}$$

where N_t is the total number of simulation time steps. From our previous investigation (Chang, Weng, and Huang, 2008), a suitable value for M is 2 million for the 2.2nm- film and 1.2 million for the 11nm- film. Figure 2 shows an example of the time-averaged temperature profile in the 11nm- thin film of length of $L_z = 128a_0$. The initial temperature ($T_{MD,i}$) is 300K. A strong nonlinearity is observed near the heat source and sink regions due to the strong scattering there. By abandoning regions within a distance of 8 nm from the center of heat source and sink regions, we take the linear fitting of the remaining parts, as shown in Fig.3, to obtain the average temperature gradient. Note the periodic boundary condition has been used to connect data at both ends. Finally, to ensure the steadiness of the system, the time evolutions of slice temperatures are monitored and a transient time period much larger than the traditional estimate $\tau = L_z^2/6D$ (Skye, Schelling, 2008) is chosen, where D is the thermal diffusivity.

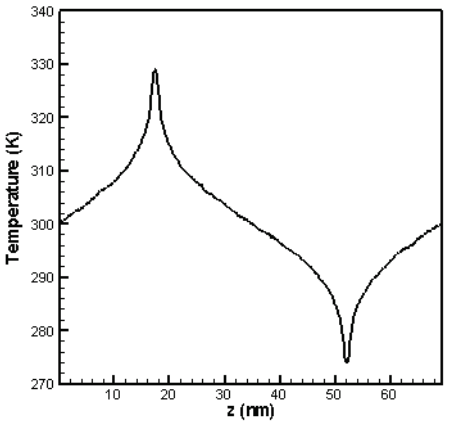

Figure 2: Time-averaged temperature profile for the 11nm- film having a length of L_z=128a_0 at $T_{MD,i}$=300K.

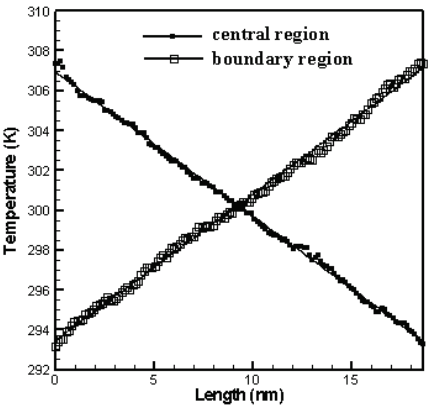

Figure 3: The linear parts of the temperature profile in the central region (z=25∼44 nm) and the boundary region (z=0∼9 nm and 60∼70 nm).

3.2 Finite-size effect

In order to obtain the thermal conductivity of infinite thin films, we adopt the extrapolation strategy suggested by Schelling, Phillpot, and Keblinski (2002). First of all, the inverse of effective mean free path Λ_{eff} is estimated by the Mattiessen's rule as follows

$$\frac{1}{\Lambda_{eff}} = \frac{1}{\Lambda_\infty} + \frac{4}{L_z} \tag{14}$$

where Λ_∞ is the mean free path of the infinite system. The factor of 4 comes from the fact that a phonon travels $L_z/4$ in between the heat source and sink regions. According to the kinetic theory, $k = CV_g\Lambda_{eff}/3$ and thus Eq.(14) can be rewritten as

$$\frac{1}{k} = \frac{3}{CV_g}\left(\frac{1}{\Lambda_\infty} + \frac{4}{L_z}\right) \tag{15}$$

where C is the specific heat and V_g is the phonon group velocity. Eq.(15) reveals a linear relationship between $1/k$ and $1/L_z$, and therefore one can extrapolate the thermal conductivity of an infinite thin film ($1/L_z \to 0$) from those of finite films.

In this study, four lengths, namely $128a_0$, $160a_0$, $192a_0$and $224a_0$, are simulated. Some results are illustrated in Fig.4. The linearity is nicely obtained. The extrapolated thermal conductivities corresponding to the infinite thin films are 18.5W/m-K and 59.2W/m-K at $T_{MD,i}$=300K as well as 11.3W/m-K and 31.6 W/m-K at $T_{MD,i}$=700K. These values however are not the final results. Quantum corrections are still needed and discussed below.

3.3 Phonon spectrum

To compute the phonon spectrum, we adopt an EMD approach or equivalently a NEMD without evoking the heat flow. All simulation parameters are the same as those used in the NEMD approach except the MD time step (0.3 fs now). Shown in Fig.5 is the MD predicted spectra of a silicon thin film of thickness 2.2 nm at $T_{MD,i}$=300K. The simulation domain chosen is $4a_0 \times 8a_0 \times 200a_0$. Compared to the bulk spectra (black curves) calculated based on the SW potential (Stillinger, Weber, 2002), discrete dispersion modes are obviously observed. Besides, their slopes, i.e. the confined phonon group velocities, are smaller than the bulk counterparts; a reduction in the thermal conductivity is thus expected. Fig.6 shows the phonon dispersion relations calculated based on the elastic continuum model (Huang, Chang, Chong, Liu, and Yu, 2007): the shear (a transverse polarization), dilatational and flexural waves (mixed polarizations). In spite of different polarizations, the analytical and simulation spectra look very similar (dilatational vs. longitudinal, flexural

vs. x-polarized transverse, and shear vs. y-polarized transverse) everywhere except near the zone boundary. Because the sample is finite, the incident waves and reflect waves near the zone boundary are merged and form standing waves, resulting in flat dispersion curves there. This phenomenon is not captured however in the elastic continuum model. Shown in Fig.7 are the phonon densities of states of the bulk Si and the Si thin films at $T_{MD,i}$=300K. The simulation domains employed are $20a_0\times20a_0\times20a_0$ for bulk Si and $4a_0\times8a_0\times200a_0$and $20a_0\times20a_0\times192a_0$ for films. Only slight difference is observed, mainly in the peak corresponding to the optical branch which seemingly decreases with decreasing film thickness. The DOS of the 11nm- film is almost indistinguishable from the bulk one.

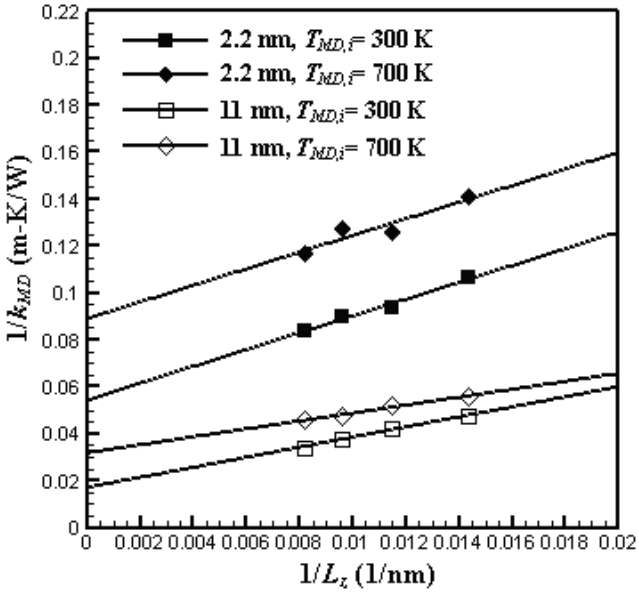

Figure 4: The linear dependence of $1/k_{MD}$ on $1/L_z$.

3.4 Quantum correction

Figure 8 shows the quantum correction results according to Eq.(10) by adopting the Debye DOS or those shown in Fig.7. In the Debye model, a linear dispersion relation is assumed and the DOS is proportion to ω^2. In Fig.8, we find that the corrected temperature is always smaller than the MD simulated temperature. The corrected temperatures based on the bulk DOS and thin film DOS are about the same and close to the corrected results (denoted as T_a in Fig.8) (Gomes, Madrid,

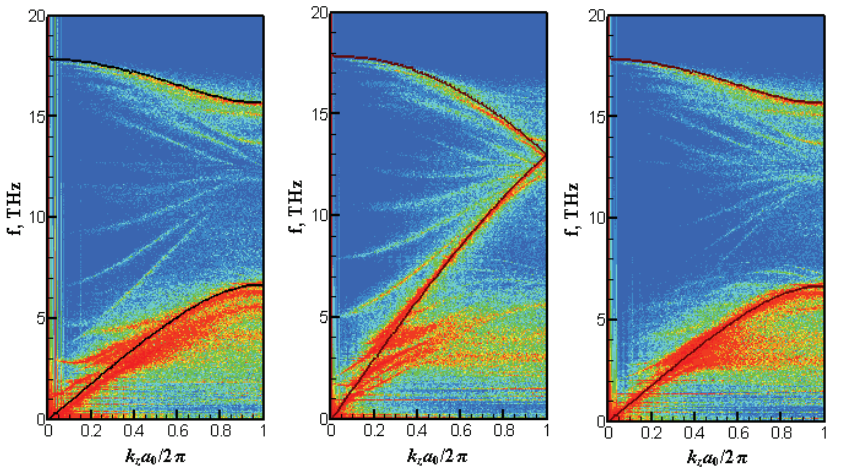

Figure 5: Phonon dispersion relations of the 2.2nm- thin film obtained by EMD: (a) longitudinal; (b) transverse (x-polarized); (c) transverse (y-polarized). The black curves are the bulk spectra.

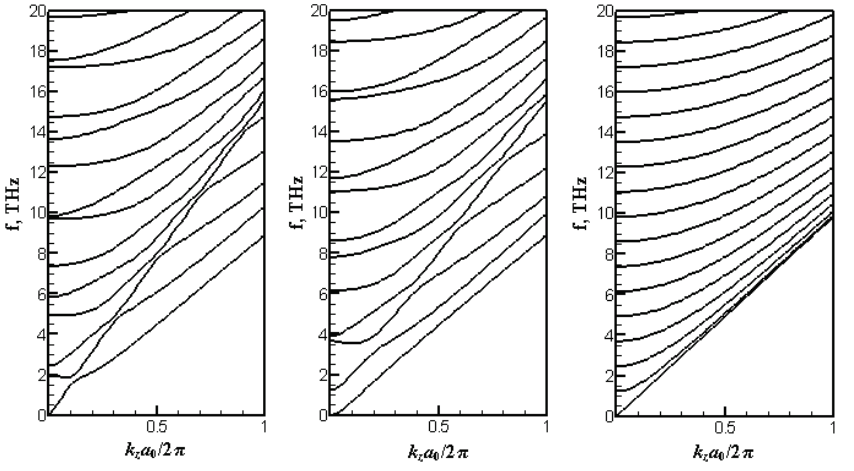

Figure 6: Phonon dispersion relations of the 2.2nm- thin film predicted by the elastic continuum model (Huang, Chang, Chong, Liu, Yu, 2007): (a) dilatational; (b) flexural; (c) shear.

Goicochea, and Amon, 2006) according to the lattice-dynamics calculation under the assumption of an isotropic continuum medium and a use of the bulk dispersion relation. Gomes, Madrid, Goicochea, and Amon (2006) also measured the bulk specific heat (C) and estimated the corrected temperature by assuming $\partial T/\partial T_{MD} = 3Nk_B/C$. The corrections (denoted as T_c in Fig.8) instead coincide with the Debye results.

Fig. 9 shows the ratio of the thermal conductivities of thin films after (k) and before (k_{MD}) the quantum correction. Note these thermal conductivities are all free from the finite-size effect. As seen, the ratio decreases and the difference between models increases with decreasing temperature and with decreasing film thickness. The Debye correction results in larger values generally. In remark, the Debye model is seemingly not a good choice for quantum correction and unless the temperature is very low (compared to the Debye temperature) or the film is very thin (compared to the phonon wavelength), a use of the bulk DOS for the quantum correction is reasonable and sufficient.

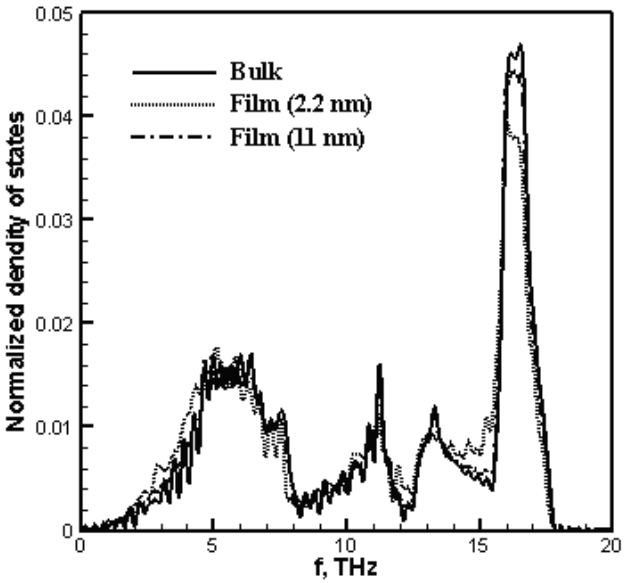

Figure 7: Phonon densities of states normalized by $3N$ obtained via EMD.

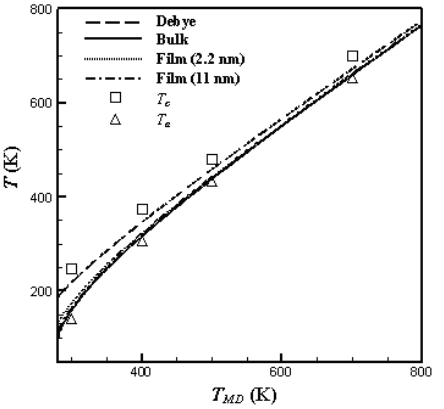

Figure 8: The quantum-corrected temperature against the MD temperature T_{MD}. T_c and T_a are the corrected results from Gomes, Madrid, Goicochea, and Amon (2006).

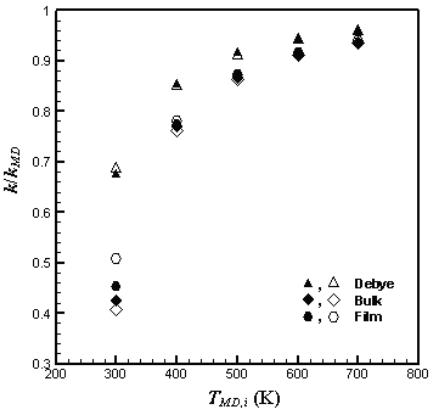

Figure 9: The ratio of the thermal conductivities after and before the quantum correction of the 11nm- thin film (solid symbols) and the 2.2nm- film (open symbols) against the $T_{MD,i}$.

3.5 Temperature dependence

We show the thermal conductivities of the 2.2nm- and 11nm- thin films against the temperature T_i (the corrected temperature of $T_{MD,i}$) in Fig. 10, compared with the theoretical predictions based on the phonon Boltzmann transport equation (Huang, Chang, Chong, Liu, and Yu, 2007). In the theoretical model, only the confined phonon spectra, the phonon-phonon scattering, and the boundary scattering are taken into consideration in order to comply with the simulation conditions. A parameter p, the fraction of phonons that are specularly reflected at the surfaces, is introduced to characterize the surface roughness. Figure 10 shows significantly reduced thermal conductivities due to the surface scattering and those of the 2.2nm-film is nearly temperature-independent as the temperature is above the room temperature. The latter implies a dominance of the surface scattering over the phonon-phonon scattering. Most of all, the thermal conductivities, free from the finite size effect and quantum corrected based on the bulk/thin film DOS, collapse excellently with the theoretical prediction of p=0.6, implying a similar surface roughness for all temperatures investigated. Because the parameters associated with the surface potential are fixed in all simulations, a similar surface roughness stands to reason. Those uncorrected or corrected by the Debye DOS nonetheless miss the theoretical variation trend with respect to the temperature. We thus conclude a quantum correction based on a proper phonon DOS is necessary in MD simulations.

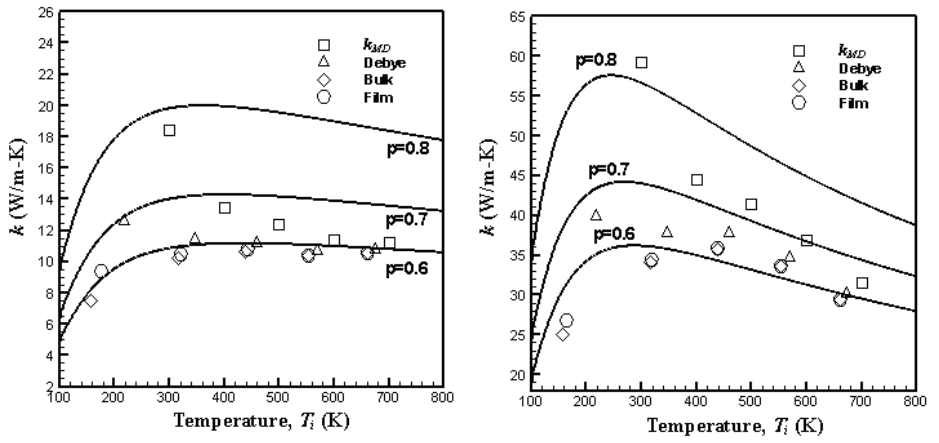

Figure 10: Thermal conductivities with or without being quantum corrected against the corrected initial temperature: (a) thickness 2.2 nm, (b) thickness 11 nm. The solid lines are theoretical predictions (Huang, Chang, Chong, Liu, Yu, 2007)

4 Conclusion

In this study, we employed the NEMD approach to calculate the in-plane thermal conductivity of silicon thin films of thickness 2.2nm and 11nm. The so-called finite-size effect was eliminated via a linear extrapolation technique. Three different phonon densities of states were tested for the quantum correction, the Debye DOS, the bulk DOS, and the thin-film DOS; the latter two were obtained via EMD. The investigation shows the thermal conductivities corrected based on the bulk DOS are very close to those corrected based on the thin-film DOS and both agree excellently with the theoretical predictions of a certain surface roughness based on the phonon Boltzmann transport equation. Those uncorrected or corrected by the Debye DOS on the other hand fail in capturing the temperature variation trend. In remark, the elimination of the finite size effect and a proper phonon DOS are both essential for obtaining accurate thermal conductivities of infinitely-long thin films and a use of the bulk phonon density of states is sufficient for the thin films and temperatures investigated herein.

Acknowledgement: This work was supported by the Industrial Technology Research Institute of Taiwan, R.O.C (project No. 97-S-A36) as well as by the National Science Council of Taiwan (Grant No. NSC 97-2221-E-002-200-MY3). We are also grateful to Computer and Information Networking Center, National Tai-

wan University, and the National Center for High-performance Computing for the support of high-performance computing facilities.

References:

Aono, M.; Hou, Y.; Oshima, C.; Ishizawa Y. (1982): Low-energy ion scattering from the Si(001) surface. *Phys. Rev. Lett.*, vol. 49, pp. 567-570.

Balandin, A.; Wang, K. L. (1998): Significant decrease of the lattice thermal conductivity due to phonon confinement in a free-standing semiconductor quantum well. *Phys. Rev. B*, vol. 58, pp. 1544-1549.

Baskes, M. I. (1987): Application of the embedded-atom method to covalent materials: A semiempirical potential for silicon. *Phys. Rev. Lett.*, vol. 59, pp. 2666-2669.

Born, M.; Oppenheimer, R. (1927): On the quantum theory of molecules. *Ann. Phys. (N.Y.)*, vol. 84, pp. 457-484.

Capinski, W. S.; Cardona, M.; Katzer, D. S.; Maris, H. J.; Ploog, K.; Ruf, T. (1999): Thermal conductivity of GaAs/AlAs superlattices. *Physica B*, vol. 263-264, pp. 530-532.

Cahilla, D. G.; Ford, W. K.; Goodson, K. E.; Mahan, G. D.; Majumdar, A.; Maris, H. J.; Merlin, R.; Phillpot, S. R. (2004): Nanoscale thermal transport. *J. Appl. Phys.*, vol. 93, pp. 793-818.

Chang, T. M.; Weng, C. C.; Huang, M. J. (2008): A NEMD study of surface roughness of silicon thin film. *Proceedings of Micronano 2008*, 70331.

Chakrabarty, A.; Cagin, T. (2008): Computational studies on mechanical and thermal properties of carbon nanotube based nanostructures. *CMC: Computer, Materials, and Continua*, vol. 7, pp. 167-190.

Che, J.; Cagin, T.; Deng, W.; Goddard, W. A. (2000): Thermal conductivity of diamond and related materials from molecular dynamics simulations. *J. Chem. Phys.*, vol. 113, pp. 6888-6900.

Chen, G. (1998): Thermal conductivity and ballistic-phonon transport in the cross-plane direction of superlattices. *Phys. Rev. B*, vol. 57, pp. 14958-14973.

Chen, W. H.; Cheng, H. C.; Hsu, Y. C. (2007): Mechanical properties of carbon nanotubes using molecular dynamics simulations with the inlayer van der Waals interactions. *CMES: Computer Modeling in Engineering and Sciences*, Vol. 20, pp. 123-146.

Dickey, J. M.; Paskin, A. (1969): Computer simulation of the lattice dynamics of solids. *Phys. Rev.*, vol. 188, pp. 1407-1418.

Feng, X. L.; Li, Z. X.; Guo, Z. Y. (2003): Molecular dynamics simulation of thermal conductivity of nanoscale thin silicon films. *Microscale Therm. Eng.*, vol. 7, pp. 153-161.

Gomes, C. J.; Madrid, M.; Amon, C. H. (2004): Thin film in-plane silicon thermal conductivity dependence on molecular dynamics surface boundary conditions. *2004 ASME International Mechanical Engineering Congress and Exposition*, pp. 345-351.

Gomes, C. J.; Madrid, M.; Goicochea, J. V.; Amon, C. H. (2006): In-plane and out-of-plane thermal conductivity of silicon thin films predicted by molecular dynamics. *J. Heat Transf.*, vol. 128, pp. 1114-1121.

Heino, P. (2007): Dispersion and thermal resistivity in silicon nanofilms by molecular dynamics. *Eur. Phys. J. B.*, vol. 60, pp. 171-179

Huang, M. J.; Chong, W. Y.; Chang, T. M. (2006): The lattice thermal conductivity of a semiconductor nanowire. *J. Appl. Phys.*, vol. 99, 114318.

Huang, M. J.; Chang, T. M.; Chong, W. Y.; Liu, C. K.; Yu, C. K. (2007): A new lattice thermal conductivity model of a thin film semiconductor. *Int. J. Heat Mass Tran.*, vol. 50, pp. 67-74.

Imamura, K.; Tanaka, Y.; Nishiguchi, N.; Tamura, S.; Maris, H. J. (2003): Lattice thermal conductivity in superlattices: molecular dynamics calculations with a heat reservoir method. *J. Phys.-Condens. Mat.*, vol. 15, pp. 8679-8690.

Jund, P.; Jullien, R. (1999): Molecular-dynamics calculation of the thermal conductivity of vitreous silica. *Phys. Rev. B*, vol. 59, pp. 13707-13711.

Khitun, A.; Balandin, A.; Wang, K. L. (1999): Modification of the lattice thermal conductivity in silicon quantum wires due to spatial confinement of acoustic phonons. *Superlattice Microst.*, vol. 26, pp. 181-193.

Kotake, S.; Wakuri, S. (1994): Molecular dynamics study of heat conduction in solid materials. *JSME Int. J. B-Fluid T.*, vol. 37, pp. 103-108.

Landry, E. S.; McGaughey, A. J. H.; Hussein, M. I. (2006): Superlattice analysis for Tailored thermal transport characteristics. *2006 ASME International Mechanical Engineering Congress and Exposition*, 13673.

Lee, Y. H.; Biswas, R.; Soukoulis, C. M.; Wang, C. Z.; Chan, C. T.; Ho, K. M. (1991): Molecular-dynamics simulation of thermal conductivity in amorphous silicon. *Phys. Rev. B*, vol. 43, pp. 6573-6580.

Jones, J. E. (1924): On the determination of molecular fields. II. From the equation of state of a gas. *Proc. Roy. Soc. A*, vol. 106, pp. 463-477.

Li, J.; Porter, L.; Yip, S. (1998): Atomistic modeling of finite-temperature properties of crystalline β-SiC. II. Thermal conductivity and effects of point defects. *J.*

Nucl. Mater., vol. 255, pp. 139-152.

Liu, D. S.; Tsai, C. Y. (2009): Estimation of thermo-elasto-plastic properties of thin-film mechanical properties using MD nanoindentation simulations and an inverse FEM/ANN computational scheme. *CMES: Computer Modeling in Engineering and Sciences*, vol. 39, pp. 29-48.

Lukes, J. R.; Li, D. Y.; Liang, X. G.; Tien, C. L. (2000): Molecular dynamics study of solid thin-film thermal conductivity. *J. Heat Transf.*, vol. 122, pp. 536-543.

McGaughey, A. J. H.; Kaviany, M. (2006): Phonon transport in molecular dynamics simulations: formulation and thermal conductivity prediction. *Advances in Heat Transfer,* Vol. 39, pp. 169-255.

Miyazaki, K.; Nagai, D.; Tsukamoto, H. (2008): Molecular dynamics simulations of heat conduction in thin film with nano-holes. *Proceedings of Micronano 2008*, 70327.

Morse, P. M. (1929): Diatomic molecules according to the wave mechanics. II. vibrational levels. *Phys. Rev.*, vol. 34, pp. 57-64.

Nair, A. K.; Farkas, D.; Kriz, R. D. (2008): Molecular Dynamics Study of Size Effects and Deformation of Thin Films due to Nanoindentation. *CMES: Computer Modeling in Engineering and Sciences*, vol. 24, pp. 239-248.

Papanicolaou, N. I.; Lagaris, I. E.; Evangelakis, G. A. (1995): Modification of phonon spectral densities of the (001) copper surface due to copper adatoms by molecular dynamics simulation. *Surf. Sci.*, vol. 337, pp. 819-824.

Plimpton, S. (1995): Fast parallel algorithms for short-range molecular dynamics. *J. Comput. Phys.*, vol. 117, pp. 1-19.

Schelling, P. K.; Phillpot, S. R.; Keblinski, P. (2002): Comparison of atomic-level simulation methods for computing thermal conductivity. *Phys. Rev. B*, vol. 65, 144306.

Skye, A.; Schelling, P. K. (2008): Thermal resistivity of Si-Ge alloys by molecular dynamics simulation. *J. Appl. Phys.*, vol. 103, 113524.

Stevens, R. J.; Zhigilei, L. V.; Norris, P. M. (2007): Effects of temperature and disorder on thermal boundary conductance at solid–solid interfaces: Nonequilibrium molecular dynamics simulations. *Int. J. Heat Mass Tran.*, vol. 50, pp. 3977-3989.

Stillinger, F. H.; Weber, T. A. (1985): Computer simulation of local order in condensed phases of silicon. *Phys. Rev. B*, vol. 31, pp. 5262-5271.

Tang, W. Z.; Advani, S. G. (2007): Non-equilibrium molecular dynamics simulation of water flow around a carbon nanotube. *CMES: Computer Modeling in*

Engineering and Sciences, vol. 22, pp. 31-40.

Tersoff, J. (1986): New empirical model for the structural properties of silicon. *Phys. Rev. Lett.*, vol. 56, pp. 632-635.

Trubitsyn, V.; Dolgusheva, E. (2007): Molecular dynamics calculations of anharmonic properties of the vibrational spectrum of BCC zirconium under pressure. *Phys. Solid State*, vol. 49, No. 7, pp. 1345-1352.

Venkatasubramanian, R.; Siivola, E.; Colpitts, T.; O'Quinn, B. (2001): Thin-film thermoelectric devices with high room-temperature Figures of merit. *Nature*, vol. 413, pp. 597-602.

Volz, S. G.; Chen, G. (1999): Molecular dynamics simulation of thermal conductivity of silicon nanowires. *Appl. Phys. Lett.*, vol. 75, pp. 2056-2058.

Volz, S. G.; Chen, G. (1999): Lattice dynamic simulation of silicon thermal conductivity. *Physica B*, vol. 263-264, pp. 709-712.

Volz, S. G.; Saulnier, J. B.; Chen, G.; Beauchamp, P. (2000): Computation of thermal conductivity of Si/Ge superlattices by molecular dynamics techniques, *Microelectr. J.*, vol. 31, pp. 815-819.

Wang, Z. H.; Li, Z. X. (2006): Research on the out-of-plane thermal conductivity of nanometer silicon film. *Thin Solid Films*, vol. 515, pp. 2203-2206.

Yim, W. M.; Paff, R. J. (1974): Thermal expansion of AIN, sapphire, and silicon. *J. Appl. Phys.*, vol. 45, pp. 1456-1457

Zhong, Z. R.; Wang, X. W.; Xu, J. (2004): Equilibrium molecular dynamics study of phonon thermal transport in nanomaterials. *Numer. Heat Tr. B-Fund.*, vol. 46, pp. 429-446.

Zou, J.; Balandin, A. (2001): Phonon heat conduction in a semiconductor nanowire. *J. Appl. Phys.*, vol. 89, pp. 2932-2938.